THE JOURNAL OF BIOLOGICAL CHEMISTRY VOL. 285, NO. 35, pp. 26806–26814, August 27, 2010

Contribution of the S5-Pore-S6 Domain to the Gating Characteristics of the Cation Channels TRPM2 and TRPM8*[S]

Received for publication, February 3, 2010, and in revised form, May 19, 2010 Published, JBC Papers in Press, June 29, 2010, DOI 10.1074/jbc.M110.109975

Frank J. P. Kühn[1], **Katja Witschas, Cornelia Kühn, and Andreas Lückhoff**

From the Institute of Physiology, Medical Faculty, RWTH Aachen University, D-52057 Aachen, Germany

The closely related cation channels TRPM2 and TRPM8 show completely different requirements for stimulation and are regulated by Ca^{2+} in an opposite manner. TRPM8 is basically gated in a voltage-dependent process enhanced by cold temperatures and cooling compounds such as menthol and icilin. The putative S4 voltage sensor of TRPM8 is closely similar to that of TRPM2, which, however, is mostly devoid of voltage sensitivity. To gain insight into principal interactions of critical channel domains during the gating process, we created chimeras in which the entire S5-pore-S6 domains were reciprocally exchanged. The chimera M2-M8P (*i.e.* TRPM2 with the pore of TRPM8) responded to ADP-ribose and hydrogen peroxide and was regulated by extracellular and intracellular Ca^{2+} as was wild-type TRPM2. Single-channel recordings revealed the characteristic pattern of TRPM2 with extremely long open times. Only at far-negative membrane potentials (−120 to −140 mV) did differences become apparent because currents were reduced by hyperpolarization in M2-M8P but not in TRPM2. The reciprocal chimera, M8-M2P, showed currents after stimulation with high concentrations of menthol and icilin, but these currents were only slightly larger than in controls. The transfer of the NUDT9 domain to the C terminus of TRPM8 produced a channel sensitive to cold, menthol, or icilin but insensitive to ADP-ribose or hydrogen peroxide. We conclude that the gating processes in TRPM2 and TRPM8 differ in their requirements for specific structures within the pore. Moreover, the regulation by extracellular and intracellular Ca^{2+} and the single-channel properties in TRPM2 are not determined by the S5-pore-S6 region.

TRPM2 and TRPM8 display the highest sequence homology within the family of transient receptor potential (TRP)[2] cation channels (1). TRPM2 is gated mostly by intracellular ADP-ribose (ADPR) and possibly by oxidative stress, for which extracellular application of hydrogen peroxide is an experimental paradigm (2, 3). ADPR binds to the intracellular NUDT9 domain, forming the C-terminal part of the TRPM2 protein (2, 4, 5). Little is known about the further details of the gating mechanism initiated after binding of ADPR; no further protein domains have been identified that mediate gating by interaction with the pore. The resulting currents of TRPM2 show a linear *I-V* relation, indicating the absence of a voltage dependence of the gating process. In contrast, TRPM8 is, in principle, a voltage-gated channel, equipped with a voltage sensor in the S4-S5 region, in analogy to voltage-gated K^+ channels (6, 7). Activation requires strongly depolarized membrane potentials. The physiological role of TRPM8 is, however, thought to be not the sensing of voltage but of cold and of some cooling agents such as menthol (1, 8, 9). It has been demonstrated that these physical and chemical stimuli shift the activation curve of TRPM8 into the negative voltage range corresponding to normal membrane potentials (6, 7). Interestingly, the S4-S5 regions of TRPM8 and TRPM2 are quite similar. In particular, all the basic amino acid residues within this region are present in TRPM2 as well as in TRPM8 (7). Therefore, we reasoned that the apparent insensitivity to voltage in TRPM2 results from differences in the pore region from S5 to S6 rather than in the voltage-sensing region. An experimental test of this hypothesis should be enabled by chimeras of TRPM2 and TRPM8 in which the respective pore regions are reciprocally exchanged. Thus, one chimera is basically a TRPM2 channel with the pore region of TRPM8, and the other is a TRPM8 channel with the pore region of TRPM2. We refer to these chimeras as M2-M8P and M8-M2P, respectively.

Furthermore, this experimental approach offers the opportunity to study the importance of the pore with respect to other functional criteria, beyond the voltage dependence. First, single-channel properties as shown in isolated patches may be essentially determined by the pore. Although the single-channel conductance of TRPM2 and TRPM8 is similar, the channel kinetics differ widely, especially in terms of the open times, which are extremely long in TRPM2 and short in TRPM8 (2, 10, 11). Of even greater functional relevance may be the question of whether regulation of the channels by intracellular and extracellular Ca^{2+} is related to the pore region. Remarkably, Ca^{2+} regulation is opposite in several aspects in TRPM2 and TRPM8. TRPM2 essentially requires extracellular Ca^{2+} for channel function (12); intracellular Ca^{2+} acts cooperatively with ADPR in channel activation (13) to an extent that, at low intracellular concentrations of ADPR, which may represent the physiological situation, the channel becomes regulated mainly by intracellular Ca^{2+} (14). In contrast, no Ca^{2+} is required for activation of TRPM8 by cold and menthol, although a distinct Ca^{2+} dependence exists for activation by another stimulus, icilin (15). Moreover, desensitization of TRPM8 channel activity is largely dependent on Ca^{2+} (16, 17), whereas TRPM2 hardly exhibits any desensitization. Extracellular binding sites for Ca^{2+}, possibly localized in the pore region, which represents

* This work was supported by Deutsche Forschungsgemeinschaft Grant DFG KU 2271/11.

[S] The on-line version of this article (available at http://www.jbc.org) contains supplemental Figs. S1 and S2.

[1] To whom correspondence should be addressed. Tel.: 49-241-808-8803; Fax: 49-241-808-2434; E-mail: fkuehn@physiology.rwth-aachen.de.

[2] The abbreviations used are: TRP, transient receptor potential; ADPR, ADP-ribose; NMDG, *N*-methyl-D-glucamine; pF, picofarads.

the main part of the protein exposed to the extracellular space, have been suggested (12, 18).

In this study, we created and functionally characterized the two reciprocal chimeras M2-M8P and M8-M2P, as well as a chimera in which the NUDT9 domain of TRPM2 was linked to the C terminus of TRPM8. The aim of this approach was to gain insight into the role of the S5-pore-S6 domain as a functional counterpart of the TRPM8 voltage sensor and the TRPM2 NUDT9 domain.

EXPERIMENTAL PROCEDURES

Molecular Cloning—The cDNAs of human *TRPM2* and *TRPM8* were subcloned into the pIRES-hrGFP-2a vector (Stratagene, La Jolla, CA). For the generation of the chimeric channels, we designed recognition sites for restriction enzymes (New England Biolabs, Beverly, MA) at corresponding positions of the open reading frame of both channels. Site-directed mutagenesis was performed using the QuikChange mutagenesis system (Stratagene). Defined oligonucleotides were obtained from MWG Biotech AG (Ebersberg, Germany). The preparation and ligation of the DNA fragments that had to be exchanged between the two channels were performed as described previously (4). After having exchanged the S5-pore-S6 domains, the original sequences at the cut-paste limits were restored. Each point mutation, as well as the correct orientation of the exchanged domains, was verified by DNA sequencing with the BigDye Terminator kit (PerkinElmer Life Sciences). To exclude the presence of inadvertent mutations in other regions of the channel, two clones with identical results were tested for each chimera or point mutant. All procedures were performed in accordance with the respective manufacturers' instructions, if not indicated otherwise.

Cell Culture and Transfection—Stable expression of wild-type and chimeric channels was achieved as follows. Each of the expression constructs, pIRES-TRPM2 and pIRES-TRPM8, and the corresponding chimeric variants were recombined with a neomycin resistance module (EC-Neo, Stratagene) according to the manufacturer's instructions. The recombination constructs were transiently transfected into HEK-293 cells (German Collection of Microorganisms and Cell Cultures, Braunschweig, Germany) using the FuGENE transfection reagent (Roche Applied Science). The transfected cells were maintained at 37 °C and 5% CO_2 in DMEM supplemented with 4 mM L-glutamine, 1 mM sodium pyruvate, and 10% (v/v) fetal calf serum and selected in the presence of G418 (gentamycin sulfate, 1 mg/ml; Invitrogen). Surviving clones that were visibly positive for the expression of enhanced green fluorescent protein were isolated and frozen at early passage numbers. These stocks were propagated in the presence of G418 (1 mg/ml) for further studies.

Electrophysiology—Whole-cell recordings were performed using a EPC 9 amplifier equipped with a personal computer with Pulse 8.5 and X Chart software (HEKA, Lambrecht, Germany).The standard bath solution contained 140 mM NaCl, 1.2 mM $MgCl_2$, 1.2 mM $CaCl_2$, 5 mM KCl, and 10 mM HEPES, pH 7.4 (NaOH). For Na^+-free solutions, Na^+ was replaced with 150 mM *N*-methyl-D-glucamine (NMDG), and the titration was performed with HCl. The divalent cation-free bath solution contained 150 mM NaCl, 10 mM EGTA, and 10 mM HEPES, pH 7.4 (NaOH). The pipette solution contained 145 mM cesium glutamate, 8 mM NaCl, 2 mM $MgCl_2$, and 10 mM HEPES, pH 7.2 (CsOH), and the Ca^{2+} concentration was adjusted either to <10 nM (10 mM CsEGTA, no Ca^{2+} addition) or to values between 1 μM and 1 mM using defined Ca^{2+} concentrations and 1 mM CsEGTA.

The Ca^{2+} concentrations of the solutions were calculated using the *MAXC* program (Stanford University). In all experiments, Cs^+ and glutamate were the main intracellular ions to minimize potential contaminating currents through K^+ and Cl^- channels. For the stimulation of TRPM2 currents, ADPR (100 mM stock solution in distilled water) was added to the intracellular solution, yielding a final concentration of 0.05–1 mM. Alternatively, TRPM2 currents were evoked by superfusion of the cells with standard bath solution containing hydrogen peroxide (30% stock solution). TRPM8 currents were induced with menthol (Sigma; 400 mM stock solution in Me_2SO) or icilin or WS-12 (Cayman Chemical; 80 mM stock solutions in Me_2SO) by application to the bath (final concentrations as indicated in the experiments). If not stated otherwise, the experiments were performed at room temperature (21 °C), and the current-voltage relations were obtained during voltage ramps from −90 to +60 mV and back to −90 mV applied over 200 ms. The holding potential was −60 mV. The stimulation by cold was performed by adding ice-cold bath solution directly to the bath chamber during measurement; the bath temperature was monitored with a digital thermometer. For analysis, maximal current amplitudes (pA) in a cell were divided by the cell capacitance (picofarads (pF)), a measure of the cell surface. The result is the current density (pA/pF).

Single-channel currents were recorded from inside-out patches at room temperature (21 °C). Patch pipettes were made of borosilicate glass (Hilgenberg GmbH, Malsfeld, Germany) and had tip resistances of between 5 and 7 megohms. Pipette tips were coated with dental wax (Moyco, Philadelphia, PA) to minimize background noise. Single-channel currents were recorded with an Axopatch 200B amplifier in combination with a Digidata 1440A AD/DA converter controlled by the pCLAMP10 software suite (Axon Instruments, Foster City, CA). A gap-free acquisition mode was used with analogous filtering at 2 kHz performed with a 4-pole Bessel filter (−3 db). External and internal solutions were the same as those used in whole-cell recordings. Patches with TRPM2 and M2-M8P were activated with ADPR (either 1 mM in Ca^{2+}-free solutions or 0.2 mM in solutions with 1 μM Ca^{2+}) added to the bath (internal) solution. Stimuli for TRPM8 were intracellular icilin (0.1–0.2 μM) and menthol (1–5 μM).

For analysis, single-channel transitions were identified on the basis of the half-amplitude threshold crossing criteria. Closed times were quantified only in patches showing exactly one active channel. Closed and open time histograms were constructed by attribution to bins of constant widths. Dwell times were fitted to a monoexponential or biexponential probability function using the built-in "compare models" algorithm of the pCLAMP10 software. Unitary current amplitudes (i_o) were determined as the difference of maxima in Gaussian fits of all-points histograms. Plots of i_o *versus* membrane voltage (V_{patch})

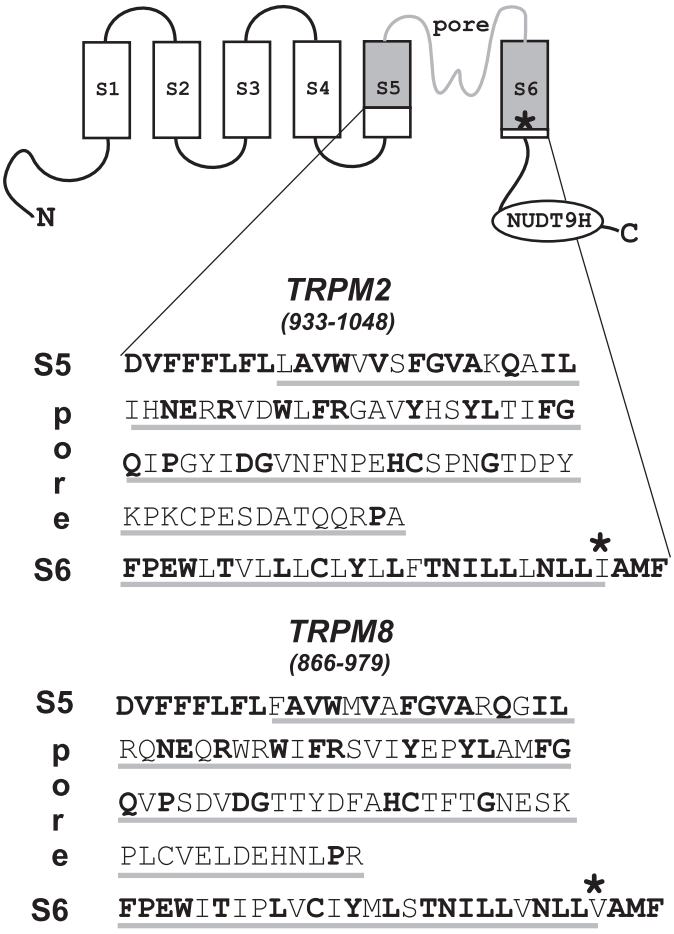

FIGURE 1. **Design of TRPM2/TRPM8 channel chimeras.** The presumed basic structure of TRP channels, including the exchanged S5-pore-S6 domain (*gray shading*), is illustrated. The corresponding amino acid sequences of TRPM2 and TRPM8 are shown in single-letter code, and conserved residues are shown in *boldface*. The site within S6 where the exchange of a hydrophobic residue with a lysine reverses the charge selectivity of the pore in both TRPM2 and TRPM8 is marked with an *asterisk* (19).

were fitted with linear regression to obtain slope conductances. Data are presented as mean ± S.E. if not indicated otherwise.

RESULTS

As illustrated in Fig. 1, we swapped two segments of TRPM2 and TRPM8 that contained 98 and 100 amino acid residues, respectively, and showed identity of ~46% altogether. The exchanged sequences contained the entire pore region, including the adjacent transmembrane segments S5 and S6, and exhibited the most pronounced homology within S5 (83%) and S6 (70%) and the less pronounced homology in the pore (30%).

Pore Exchange of TRPM2 Does Not Change Gating—First we studied the chimera M2-M8P (TRPM2 channel containing the S5-pore-S6 domain of TRPM8) with respect to its activation, single-channel properties, and requirements for Ca^{2+}. It should be noted that this chimera differs from a previously characterized one that was anion-selective due to the single amino acid exchange I1045K (indicated in Fig. 1) (19). In whole-cell experiments with ADPR (0.05–0.6 mM) added to the pipette fluid or after extracellular stimulation with 10 mM hydrogen peroxide, this chimera displayed cation-selective currents with a linear *I-V* relation that were readily blocked in the inward direction by NMDG. No difference was noted in comparison with wild-type TRPM2 (Figs. 2–4). No currents were evoked ($n = 4$) by the typical stimuli of TRPM8, menthol (up to 0.2 mM) and cold (6 °C). Removal of Ca^{2+} from both sides of the cell membrane completely abolished any currents both through TRPM2 and M2-M8P (Fig. 2). When the intracellular fluid contained 1 μM Ca^{2+}, removal of extracellular Ca^{2+} inhibited the currents as well. However, the inhibition was considerably slower (Fig. 3). The t_{90} of current decline in wild-type TRPM2 was 16 ± 1.5 s ($n = 4$) in the presence and 2.8 ± 1.0 s ($n = 6$) in the absence of intracellular Ca^{2+}. The corresponding t_{90} values of the M2-M8P chimera were 22 ± 3.6 s ($n = 5$) and 3.5 ± 0.9 s ($n = 4$). Therefore, the kinetics of current decline after extracellular Ca^{2+} depletion were nearly identical in both channels. In both cases, the replenishment of extracellular Ca^{2+} led to a complete recovery of currents through TRPM2 and M2-M8P (Figs. 2 and 3). It has been proposed that TRPM2 does not necessarily require ADPR for its activation when extremely high levels of intracellular Ca^{2+} are present (20). In our hands, however, these results could not be reproduced. Even with Ca^{2+} concentrations of 0.25 and 1 mM in the pipette fluid, no current activation was observed either in cells expressing wild-type TRPM2 ($n = 6$) (Fig. 4*A*) or in cells expressing the M2-M8P chimera ($n = 5$) (Fig. 4*B*). As a control, we demonstrated that the cells that proved nonresponsive to Ca^{2+} alone were capable of producing normal TRPM2 currents when exposed to 10 mM hydrogen peroxide. As a known stimulus of TRPM2 and in contrast to ADPR, hydrogen peroxide is effective when applied to the extracellular side of the cell membrane. Fig. 4 (*A–C*) shows the typical hydrogen peroxide-stimulated currents of wild-type TRPM2 and M2-M8P appearing after a characteristic delay of 2–4 min.

The single-channel properties of M2-M8P were studied in inside-out patches and compared with those of wild-type TRPM2 and TRPM8 (Fig. 5). The standard holding potential was −60 mV. When TRPM8 was stimulated with icilin (0.1 μM), characteristic channel openings were observed with durations that allowed the determination of unitary current amplitudes and of the channel conductance (Fig. 5*A*). In contrast, in the presence of menthol (1–2 μM), only extremely short openings appeared that could hardly be resolved at the standard filtering rate of 2 kHz (Fig. 5*A*). A detailed analysis indicated that the openings in the presence of icilin had a conductance of 63 ± 2 picosiemens and a mean open time of 1.31 ± 0.04 ms; additionally, a component of shorter openings was present with a mean open time of 0.21 ± 0.01 ms. This shorter component was completely predominant under basal conditions (at room temperature; data not shown) as well as in the presence of menthol (Fig. 5*A*). Channel openings of wild-type TRPM2 revealed a completely different pattern, although the single-channel conductance (64 ± 2 picosiemens) was almost identical to that of TRPM8. Channel openings of TRPM2 were extremely long, and the open probability in the presence of ADPR (200 μM) and Ca^{2+} (1 μM) on the cytosolic face of the patch approached 1 (Fig. 5*B*). The mean open time was calculated as 296 ± 12 ms, exceeding that of TRPM8 by >2 orders of magnitude. The M2-M8P chimera displayed channel openings that were virtually identical to those of wild-type TRPM2. In particular, the

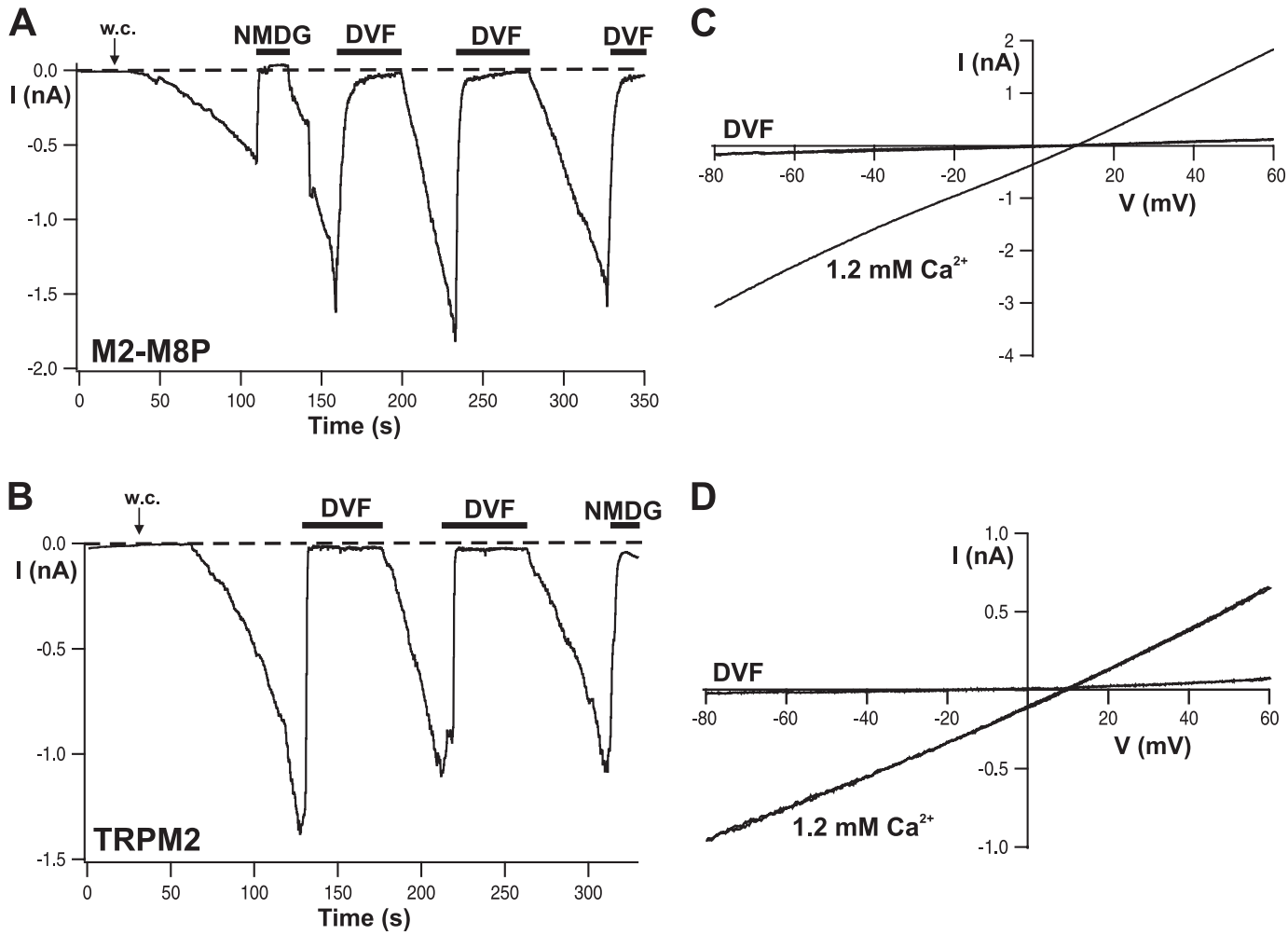

FIGURE 2. **Activation of M2-M8P by ADPR and regulation by extracellular Ca^{2+}.** *A* and *B*, whole-cell (*w.c.*) currents of cells expressing M2-M8P and wild-type TRPM2, respectively, elicited by infusion of 0.6 mM ADPR through the patch pipette. Each example represents four to five similar experiments. The Ca^{2+} concentration of the pipette solution was buffered with EGTA to below 10 nM. *Horizontal black bars* indicate time periods during which the standard bath solution (1.2 mM Ca^{2+}) was exchanged with either a divalent cation-free solution (*DVF*) or a solution containing NMDG as the main extracellular cation. *C* and *D*, *I-V* relations of currents shown in *A* and *B*, respectively, obtained during voltage ramps from −90 to +60 mV from a holding potential of −60 mV.

mean open time was 293 ± 11 ms (Fig. 5*C*). The single-channel conductance of the M2-M8P chimera was similar as in the case of the two parental channels (supplemental Fig. S1). Thus, the typical channel properties of TRPM2 were left unaltered after the exchange of the pore.

TRPM8 Pore Transfers Some Voltage Sensitivity to TRPM2—For TRPM8, an essentially voltage-dependent gating mechanism is well established (6, 7). However, the putative voltage sensor of TRPM8 is well conserved in TRPM2, although this channel is largely insensitive to membrane voltage (2, 7). We reasoned that the original S5-pore-S6 region of TRPM8 may contain a critical counterpart or extension of the voltage sensor in S4-S5. Accordingly, the insertion of the TRPM8 pore might transfer some kind of voltage sensitivity to TRPM2. Indeed, there was a slight change in the *I-V* curve (Fig. 6*A*) at strongly hyperpolarized potentials, more negative than usually applied during voltage ramps. Current amplitudes were no longer enhanced but rather decreased when potentials more negative than −120 mV were applied, especially when the currents were developing during infusion of ADPR in the beginning of whole-cell experiments. To test how this *I-V* behavior is reflected in single-channel analysis, we applied voltage steps from −60 to −120 or −150 mV (or up to 120 mV as a control) to inside-out patches from TRPM2 and M2-M8P activated with ADPR (Fig. 6, *B* and *C*). In control experiments with TRPM2, the long openings were not influenced by the holding potentials. In contrast, strongly reduced open probabilities were evoked in M2-M8P by far-negative potentials. This was due to frequent channel closures of sizeable duration not seen at control holding potentials. Specifically, wild-type TRPM2 had a mean closure time of ~0.22 ms at −60, −120, and −140 mV (for details, see Fig. 7). M2-M8P had a mean closure time in the same range at −60 mV. However, a second component of 3 ms appeared at −120 mV; the weight of this component was increased from 24 to 70% when the holding potential was more strongly hyperpolarized to −140 mV. Therefore, the flattening of the *I-V* curve in whole-cell experiments of M2-M8P is explained by a component of long single-channel closings induced by strongly negative membrane potentials. Single-channel unitary conductance was not reduced by hyperpolarization (data not shown). Thus, if the *I-V* relation is considered over a wide range, M2-M8P produces larger currents at more positive voltages, in principle

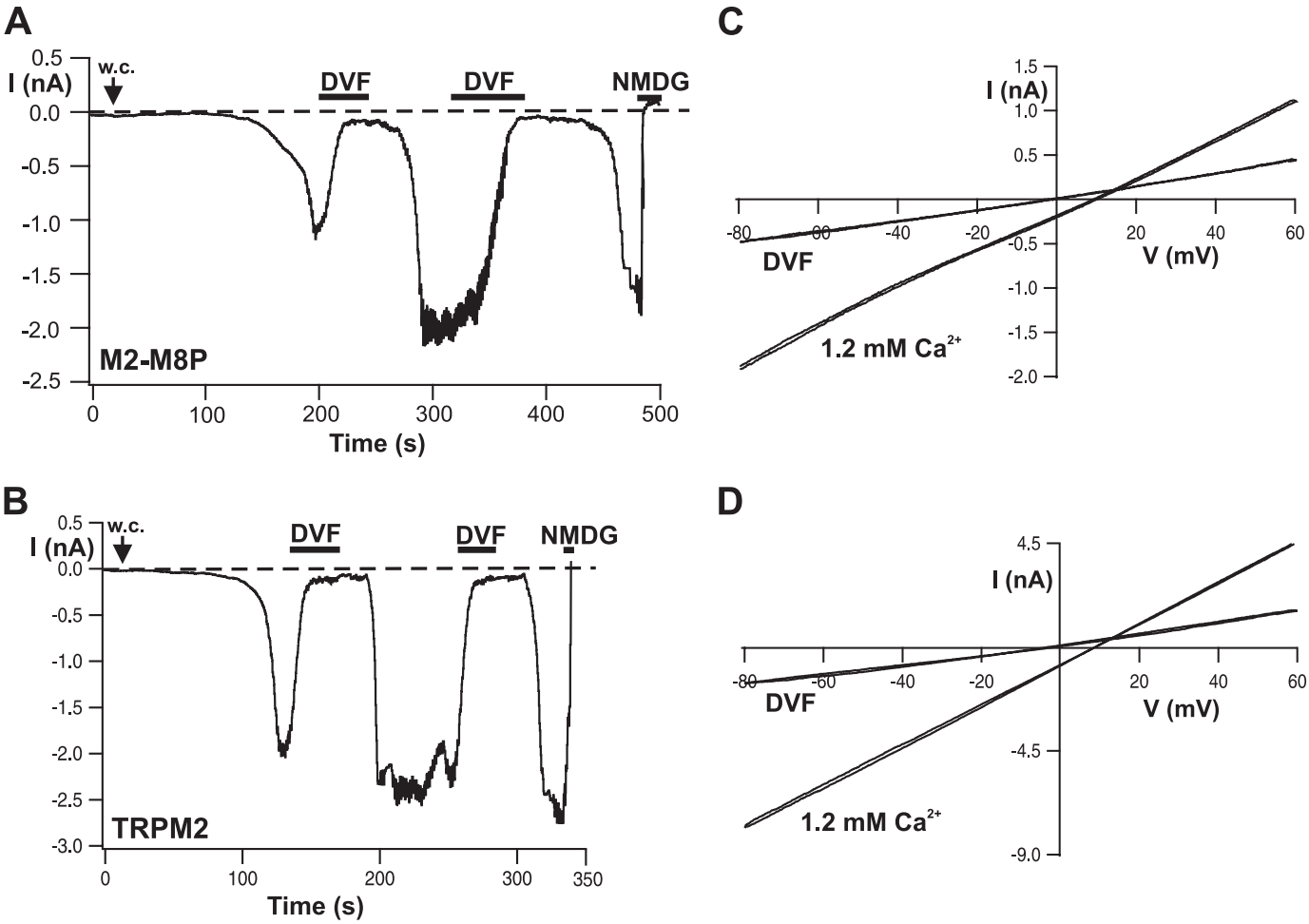

FIGURE 3. **Inhibition of wild-type TRPM2 and M2-M8P by divalent cation-free extracellular solution but in the presence of 1 μM intracellular Ca^{2+}.** *A* and *B*, whole-cell (*w.c.*) currents of cells expressing M2-M8P and wild-type TRPM2, respectively. Each example represents four to six similar experiments. Currents were elicited by infusion of ADPR (0.05 mM) and Ca^{2+} (1 μM) through the patch pipette. The holding potential was −30 mV to attenuate the large currents. Note the delayed response of current inhibition during Ca^{2+} depletion and the renewed current development during replenishment of extracellular Ca^{2+}. The kinetics of inhibition were analyzed and are reported in text. *Horizontal black bars* indicate time periods during which the standard bath solution (1.2 mM Ca^{2+}) was exchanged with either a divalent cation-free solution (*DVF*) or a solution containing NMDG as the main extracellular cation. *C* and *D*, *I-V* relations of currents shown in *A* and *B*, respectively, obtained during voltage ramps from −90 to +60 mV from a holding potential of −60 mV.

similar to wild-type TRPM8 but clearly different from wild-type TRPM2.

Pore Exchange of TRPM8 Dramatically Decreases Activation—The reverse chimera M8-M2P, in which a TRPM8 channel was substituted with the entire S5-pore-S6 domain of TRPM2 (Fig. 1), was studied under conditions previously established to induce currents in wild-type TRPM8 (*e.g.* Ref. 21). TRPM8 can be activated by menthol and some menthol derivatives, by icilin, and by cold temperatures (1, 8, 22). In M8-M2P, there was no current induction when the chemical stimuli were applied in standard concentrations or when cooling was performed to 6 °C. We then applied menthol and icilin in combination and in very high concentrations (0.5–1 mM and 60–120 μM, respectively). Unfortunately, control cells (native HEK cells) displayed significant currents under these conditions, which were slow in development, blocked by NMDG (supplemental Fig. S2*A*), and inhibited by *N*-(*p*-amylcinnamoyl)-anthranilic acid (data not shown). The current density was 20.4 ± 3.9 pA/pF at −60 mV (n = 8). In HEK cells transfected with M8-M2P, the current density was 46.5 ± 4.4 pA/pF at −60 mV (n = 21) in the presence of menthol and icilin, which was significantly larger (Wilcoxon signed rank test, p = 0.0039) but only by a factor of ~2. As in controls cells, current development was slow, in contrast to the rapid effects of the stimuli on wild-type TRPM8 (*e.g.* Ref. 17), but sensitive to NMDG and *N*-(*p*-amylcinnamoyl)anthranilic acid (data not shown) and removed by washout of the stimulus menthol (supplemental Fig. S2*B*). For comparison, the current density of wild-type TRPM8 after stimulation with 200 μM menthol or 30 μM icilin was 306 ± 30 pA/pF at −60 mV (n = 10). Because native HEK cells exhibit variable outward currents, probably related to volume-sensitive chloride channels, the outward component of currents through M8-M2P could not be analyzed in a meaningful way. Taken together, the results show that the insertion of the pore of TRPM2 into TRPM8 channels dramatically reduces if not abolishes channel function.

The NUDT9 Domain Does Not Directly Interact with the Pore Domain—It is unknown whether the NUDT9 domain of TRPM2 interacts with the channel pore as suggested for the voltage sensor in the case of TRPM8. To address this experi-

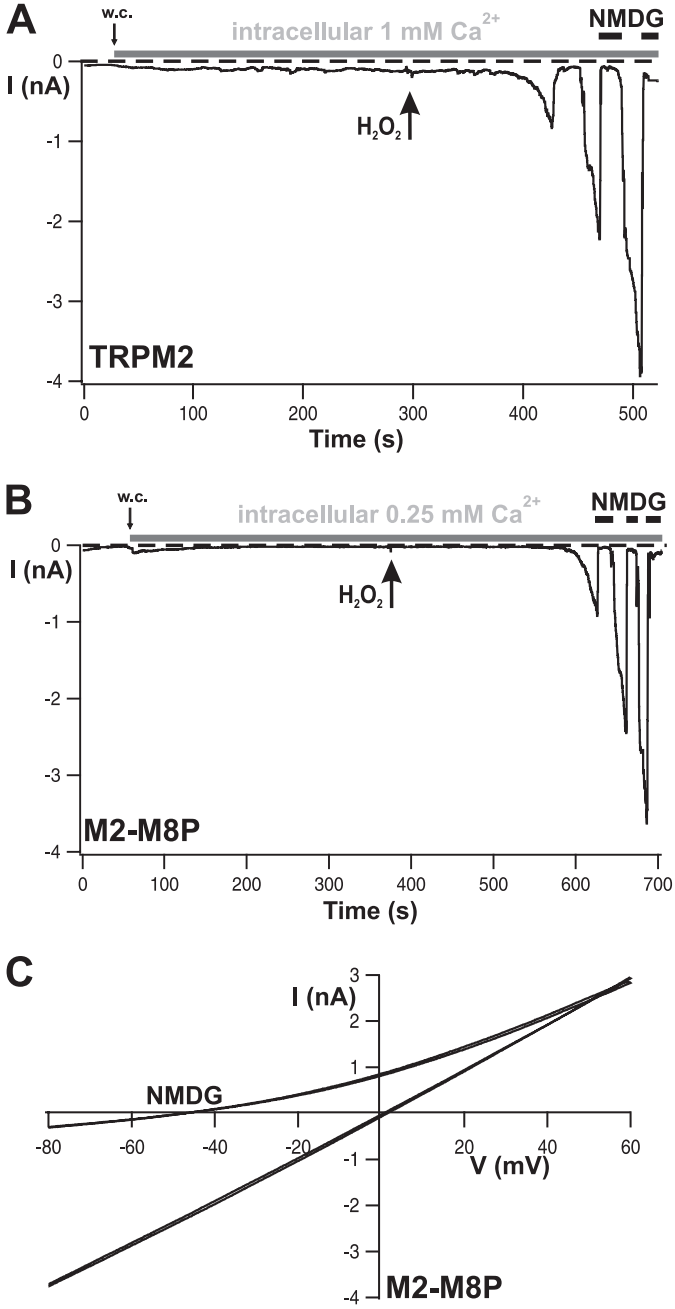

FIGURE 4. **M2-M8P and wild-type TRPM2 are not stimulated by intracellular Ca^{2+} alone but by extracellular hydrogen peroxide.** *A* and *B*, whole-cell (*w.c.*) currents of cells expressing wild-type TRPM2 and M2-M8P, respectively, recorded in the presence of high concentrations of Ca^{2+} in the patch pipette (*horizontal gray bars*, concentrations as indicated). Hydrogen peroxide (10 mM) was applied to the extracellular (bath) solution as marked by *arrows*. *C*, *I-V* relations of currents shown in *B*.

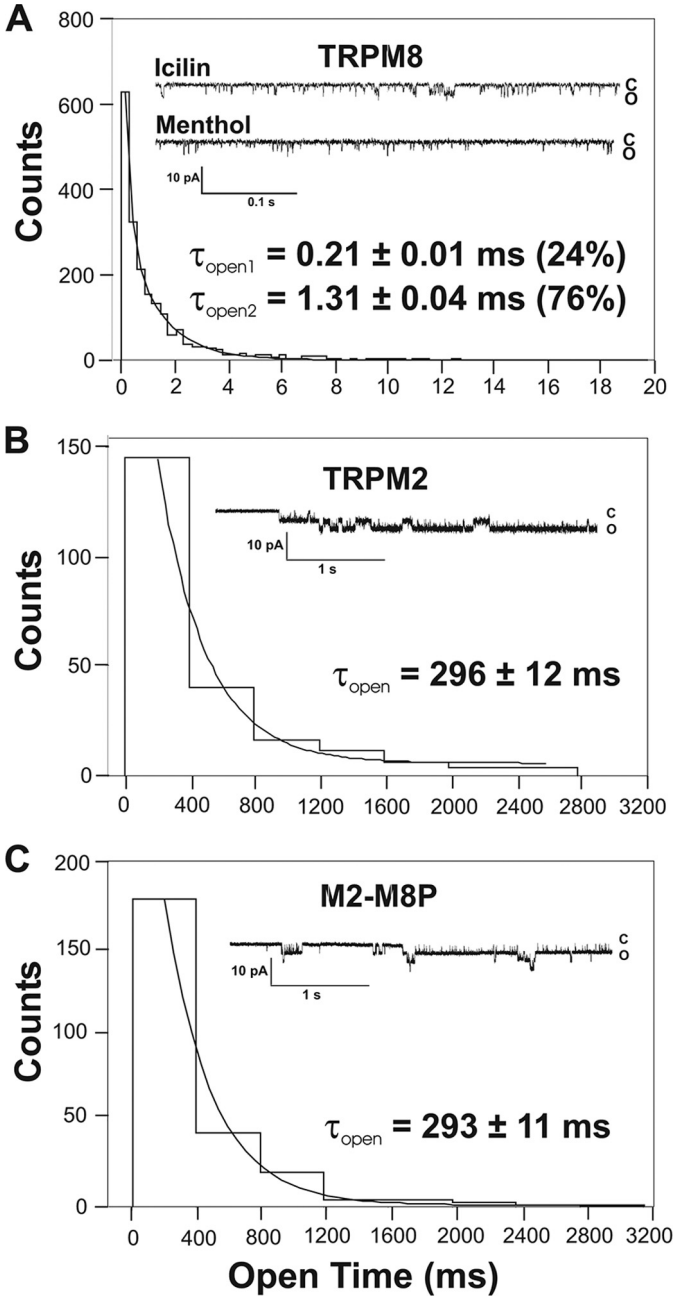

FIGURE 5. **Comparison of the single-channel kinetics of TRPM2, TRPM8, and M2-M8P.** *A*–C show representative traces from inside-out patches from cells transfected with wild-type TRPM8, wild-type TRPM2, or M2-M8P, respectively, along with an analysis of the open times. The number of openings was attributed to bins of widths shown on the *abscissa*. Mono- or biexponential fits of the histograms yielded the open times (τ_{open}) indicated for each panel. The holding potential was −60 mV. Data were sampled from a total of 12 patches. *c*, closed; *o*, open.

mentally, we transferred the NUDT9 domain, including the preceding linker of 68 amino acid residues, to the C terminus of TRPM8 (Fig. 8*A*). This linker, absent in TRPM8, should ensure that the distance between the NUDT9 domain and domains is preserved. In whole-cell patch-clamp experiments with this chimera (M8M2-nud), no obvious differences from wild-type TRPM8 were noted with respect to voltage dependence, cold sensitivity, and sensitivity to chemical agonists such as the menthol analog WS-12 (Fig. 8, *B* and *C*) (17). On the other hand, even after prolonged infusion of the cells with 1 mM ADPR together with 1 μM Ca^{2+}, there was no current activation at any holding potential ($n = 5$).

DISCUSSION

The two channels TRPM2 and TRPM8 are closely related but gated by quite different mechanisms. As a main finding of this study, we report that the gating of TRPM8, mediated by the voltage sensor and largely facilitated by specific stimuli, critically depends on the pore region between S5 and S6. This is

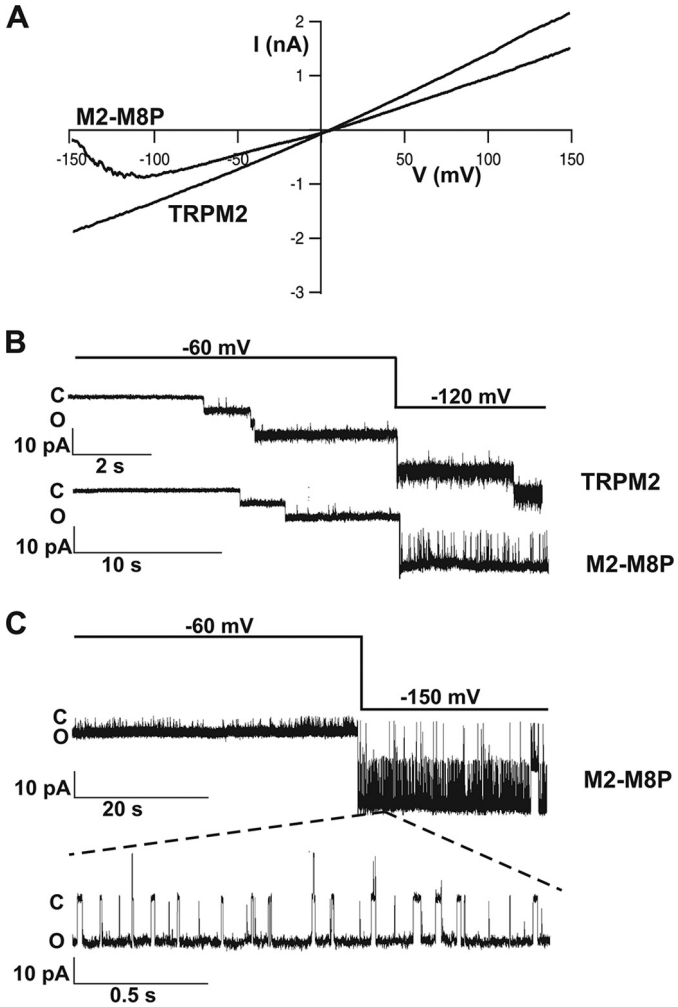

FIGURE 6. **Behavior of M2-M8P at far-negative potentials.** *A*, current-voltage relation of M2-M8P and TRPM2 obtained with voltage ramps from −150 to +150 mV. *B* and *C*, increased closed times of M2-M8P at strong hyperpolarization. *B* shows characteristic traces from TRPM2 (*upper*) and M2-M8P (*lower*) during activation by ADPR (0.1 mM in 1 μM Ca^{2+}). After the opening of several channels, the holding potential was changed from −60 to −120 mV. *C* shows the effects of hyperpolarization to −150 mV of ADPR-activated M2-M8P at two different time scales.

demonstrated by the almost complete loss of function of the M8-M2P chimera, in which the pore of TRPM2 was inserted into TRPM8. In contrast, the gating initiated by binding of ADPR to the NUDT9 domain of TRPM2 is versatile with respect to the required properties of the pore because the M2-M8P chimera behaved almost identically to wild-type TRPM2. Only at extremely negative holding potentials did the pore of TRPM8 confer some voltage sensitivity to TRPM2. As a further major finding, the single-channel properties of TRPM2 were completely preserved after the exchange of the pore with that of TRPM8, indicating that characteristic channel features like mean open and closed times are determined mainly by gating rather than by specific pore properties. Finally, regulation by extracellular and intracellular Ca^{2+} of TRPM2 and M2-M8P was identical, ruling out that the pore governs the opposite sensitivity to Ca^{2+} in TRPM2 and TRPM8.

This opposite regulation by Ca^{2+} of TRPM2 and TRPM8 is most evident when activation of TRPM8 by menthol and cold is compared with that of TRPM2 by ADPR. Menthol and cold are effective in the presence and absence of Ca^{2+} alike, and Ca^{2+} removal may even enhance currents (15, 17, 23, 24). Conversely, there is a strict cooperative effect of intracellular Ca^{2+} in the ADPR-dependent activation of TRPM2 (2, 13). At low micromolar and submicromolar concentrations of ADPR, TRPM2 becomes a Ca^{2+}-activated channel (12, 14). It has even been proposed that intracellular Ca^{2+} alone is sufficient to fully activate TRPM2 at concentrations exceeding 50 μM (20), although these findings could not be reproduced in this study and are not supported by the results of other groups (*e.g.* Ref. 18). In the same line, we did not find Ca^{2+}-induced activation of TRPM2 currents in neutrophil granulocytes when ADPR was removed from the cytosol by an ADPR-free pipette solution (14). Notwithstanding, the positive role of Ca^{2+} in the activation of TRPM2 is clearly established, involving extracellular as well as intracellular Ca^{2+}. For example, activated TRPM2 currents were inhibited during exposure of the cells to Ca^{2+}-free bath solution containing Ca^{2+} chelators (12). In our hands, the kinetics but not the amount of this effect were dependent on the presence of intracellular Ca^{2+}. Importantly, binding sites for Ca^{2+} have been proposed within the intracellular as well as the extracellular face of the TRPM2 pore (12, 18). However, our experiments reveal that Ca^{2+} regulation cannot be localized within the S5-pore-S6 domain because the characteristic hallmarks of regulation by Ca^{2+} of wild-type TRPM2 were fully conserved in M2-M8P, contrasting with the converse regulation by Ca^{2+} of wild-type TRPM8.

Characteristic channel properties that can be used in single-channel analysis as "fingerprint" markers include channel amplitudes, open times, closed times, and voltage dependence. The single-channel amplitudes in TRPM2 and TRPM8 are so similar (2, 11) that they can hardly be distinguished; therefore, it is not surprising that M2-M8P exhibited the same conductance as well. However, open times differ by >2 orders of magnitude between TRPM2 and TRPM8. The openings of TRPM2 are extraordinarily long and interrupted by very short closures, resulting in an open probability of almost 1 (2, 10). Because of the high open probability and short duration of the closures, the results of a mean open time analysis depend critically on the definition of a closure that is considered to interrupt an opening; with filter rates that suppress the detection of short closures, mean open times of several seconds can be obtained. The unique behavior of TRPM2 channels may be a consequence of unique gating mechanisms initiated by ADPR binding to the NUDT9 domain. Single-channel studies on M2-M8P revealed the same pattern as in TRPM2, characterized by long open times with only a few and short closures. Therefore, our experiments clearly demonstrate that the open time of TRPM2 does not represent an intrinsic property of the pore; rather, processes outside of the pore determine the kinetics of pore openings and closings.

The classical voltage sensors of voltage-gated cation channels have 5–7 cationic arginine or lysine residues at every third position, with hydrophobic and nonpolar residues between. This pattern is strongly conserved among the known voltage-gated Na^+, K^+, and Ca^{2+} channels (*e.g.* reviewed in Refs. 25 and 26). For voltage-sensitive TRP channels, especially TRPM8, TRPV1, and TRPA1, a rudimentary voltage sensor was postu-

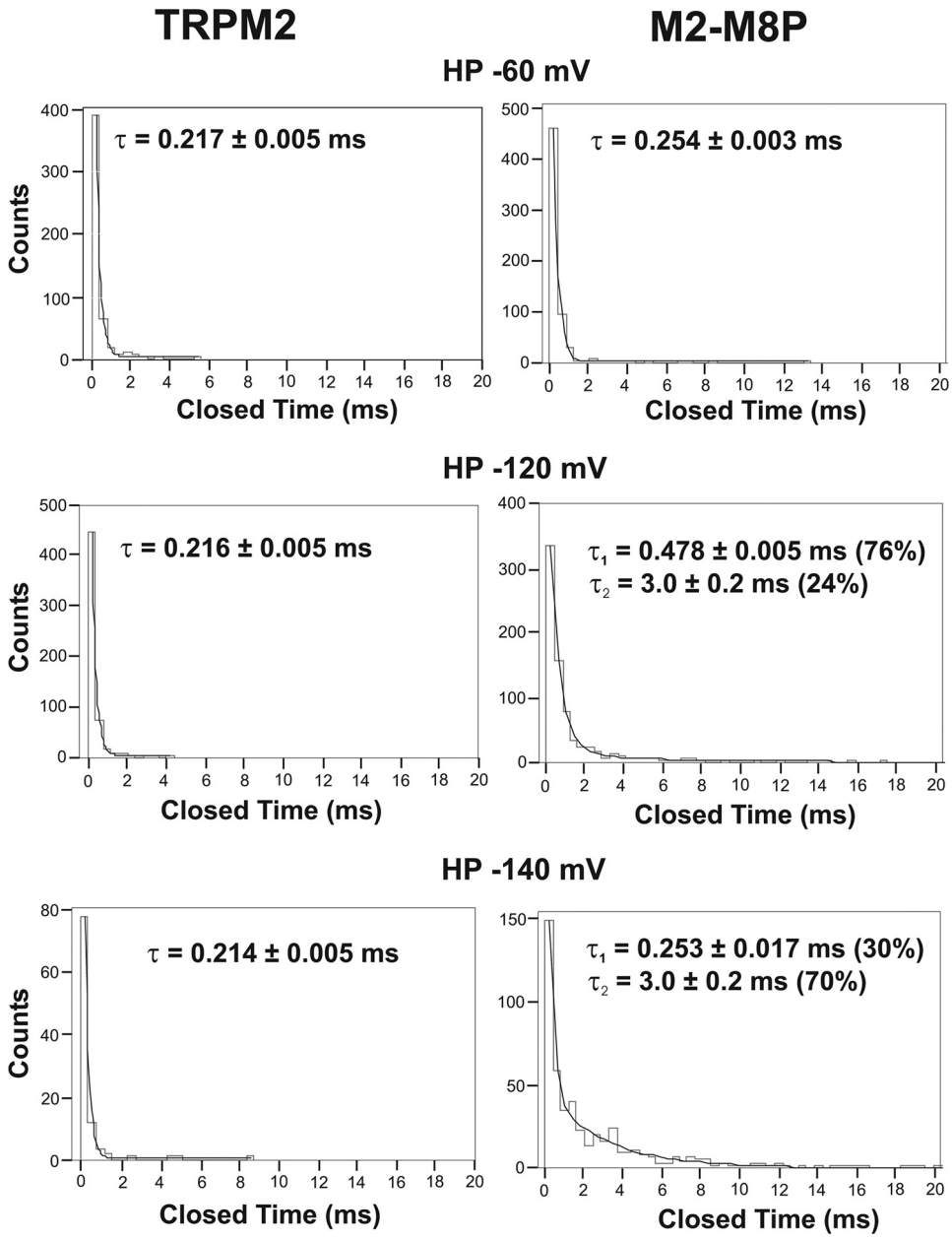

FIGURE 7. **Closed times of wild-type TRPM2 and M2-M8P are different at far-negative holding potentials.** The duration of closings was attributed to bins and counted. The distribution could be well fitted to a mono-exponential function in the case of TRPM2 (*left panels*), yielding a single τ similar for each holding potential (*HP*; −60, −120, and −140 mV). In the case of M2-M8P (*right panels*), a fit to a biexponential function was required at the two more negative potentials, yielding a second τ, which contributed 24% at −120 mV and 70% at −140 mV. Data are from a total of 14 patches for each channel.

lated. In particular, TRPM8 shows a regular pattern of lysine and arginine residues within S4 and the S4-S5 linker (6, 7, 27). The voltage dependence of TRPM8 is especially predominant at low levels of activation, *e.g.* as induced by cooling from 36 to 20 °C. It has been demonstrated by Voets *et al.* (6, 7) that activation of TRPM8 by cold as well as by menthol involves a shift in the voltage dependence of the channel, resulting in dramatically reduced energies required for activation. It has been proposed that the underlying mechanism involves interaction of a voltage sensor in the S4-S5 region with the pore region (28, 29). These data demonstrate that this interaction depends in a critical way on specific structures in the pore. With the pore of TRPM2, the interaction takes place with a strongly reduced effectivity, if at all. The M8-M2P chimera exhibited currents only at extremely high concentrations of menthol and icilin; these currents were slow in onset and could be distinguished from similar currents in control cells only by statistical means, precluding further detailed biophysical analysis.

Wild-type TRPM2 is largely devoid of voltage dependence; only a voltage-dependent deactivation has been described (2). Interestingly, the S4-S5 region in TRPM2 contains the same pattern of positively charged residues as the homologous region in TRPM8 that is considered the voltage sensor. This sensor enables channel openings of TRPM8 at positive potentials, whereas opening is obstructed at negative ones. In principle, this phenomenon was observed in M2-M8P as well, even though the relevant voltage range was considerably shifted to the left. The data would be in line with the idea that there is a voltage-sensing domain in TRPM2 as well; however, this domain is dysfunctional under normal conditions because of lack of a suitable counterpart in the native pore.

Although the role of the voltage sensor in the gating of TRPM8 is well established, it is unknown how gating is achieved in TRPM2 after binding of ADPR to the NUDT9 domain. If NUDT9 interacted directly with the pore, the results on M2-M8P would indicate that this interaction could take place with the pore of TRPM8 as well. However, the extension of TRPM8 with the NUDT9 domain failed to convey the capability to develop ADPR-induced currents, although it did not noticeably change the sensitivity to cold and chemical agonists. Therefore, there is no support for the hypothesis of a direct interaction of the NUDT9 domain with the pore. Thus, other gating mechanisms distinct from that of TRPM8 seem to take place in TRPM2 involving yet unidentified further domains. It has been proposed that calmodulin-binding sites in the N terminus of TRPM2 play a decisive role (30). In our hands, cytosolic Ca^{2+} alone even at concentrations up to 2 orders of magnitudes above physiological ranges did not activate TRPM2 or M2-M8P, whereas ADPR was effective despite intracellular EGTA concentrations of 10 mM, sug-

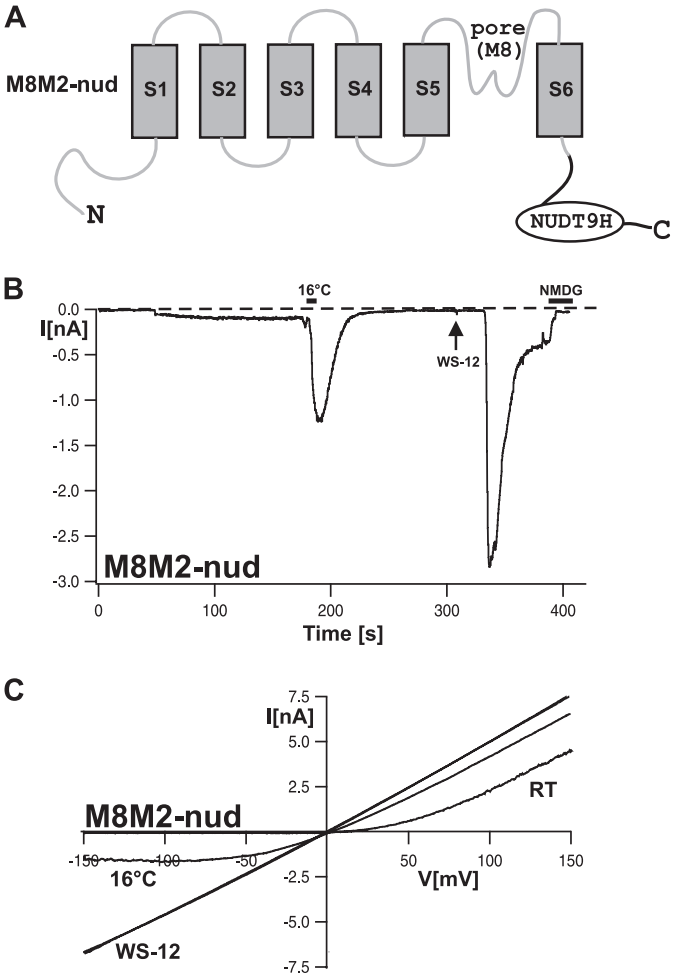

FIGURE 8. **Whole-cell patch-clamp analysis of the M8M2-nud chimera.** *A*, illustration of the channel structure of the M8M2-nud chimera, in which the NUDT9 domain of TRPM2 was C-terminally linked to TRPM8 (amino acids 1097–1104 of TRPM8 were replaced with amino acids 1168–1503 of TRPM2). *B*, whole-cell currents of a cell expressing M8M2-nud. The pipette solution contained 1 mM ADPR and 1 μM Ca^{2+}. After infusion of ADPR and Ca^{2+} for >2 min did not induce currents, the cell was exposed to ice-cold bath solution for ~10 s (as indicated by the *horizontal black bar*) and then stimulated with the menthol analog WS-12 (30 μM; *arrow*). The example shown is representative of five similar experiments. *C*, *I-V* relation of currents shown in *B* obtained during voltage ramps from −150 to +150 mV from a holding potential of −60 mV. *RT*, room temperature.

gesting that activation does not essentially require contribution of calmodulin binding.

In conclusion, the exchange of the S5-pore-S6 domain had remarkably few effects on TRPM2. In particular, single-channel properties and regulation by Ca^{2+} were completely independent of this domain. The fact that the activation of M2-M8P and wild-type TRPM2 by ADPR was almost identical, whereas the voltage-dependent activation of M8-M2P was nearly abolished, illustrates the presence of different gating mechanisms for TRPM2 and TRPM8. Evidence has been presented that TRPM8 has evolutionarily developed from an ancestral type of a TRPM2-like channel (31); this process involved not only loss of the C-terminal Nudix domain but also the switch to a different gating mechanism. The potential of pore domains to respond to various gating scenarios after mild structural modifications may be an important prerequisite for the development of the extremely broad spectrum of different activation mechanisms and biological roles characteristic for the TRP family.

Acknowledgments—We thank Dr. Veit Flockerzi (University of Homburg, Homburg, Germany) for the cDNA of human TRPM8. We also thank Hannelore Heidtmann, Ilinca Ionescu, and Barbara Poser for expert technical assistance.

REFERENCES

1. Peier, A. M., Moqrich, A., Hergarden, A. C., Reeve, A. J., Andersson, D. A., Story, G. M., Earley, T. J., Dragoni, I., McIntyre, P., Bevan, S., and Patapoutian, A. (2002) *Cell* **108,** 705–715
2. Perraud, A. L., Fleig, A., Dunn, C. A., Bagley, L. A., Launay, P., Schmitz, C., Stokes, A. J., Zhu, Q., Bessman, M. J., Penner, R., Kinet, J. P., and Scharenberg, A. M. (2001) *Nature* **411,** 595–599
3. Hara, Y., Wakamori, M., Ishii, M., Maeno, E., Nishida, M., Yoshida, T., Yamada, H., Shimizu, S., Mori, E., Kudoh, J., Shimizu, N., Kurose, H., Okada, Y., Imoto, K., and Mori, Y. (2002) *Mol. Cell* **9,** 163–173
4. Kühn, F. J., and Lückhoff, A. (2004) *J. Biol. Chem.* **279,** 46431–46437
5. Perraud, A. L., Takanishi, C. L., Shen, B., Kang, S., Smith, M. K., Schmitz, C., Knowles, H. M., Ferraris, D., Li, W., Zhang, J., Stoddard, B. L., and Scharenberg, A. M. (2005) *J. Biol. Chem.* **280,** 6138–6148
6. Voets, T., Droogmans, G., Wissenbach, U., Janssens, A., Flockerzi, V., and Nilius, B. (2004) *Nature* **430,** 748–754
7. Voets, T., Owsianik, G., Janssens, A., Talavera, K., and Nilius, B. (2007) *Nat. Chem. Biol.* **3,** 174–182
8. McKemy, D. D., Neuhausser, W. M., and Julius, D. (2002) *Nature* **416,** 52–58
9. Reid, G., Babes, A., and Pluteanu, F. A. (2002) *J. Physiol.* **545,** 595–614
10. Heiner, I., Eisfeld, J., Halaszovich, C. R., Wehage, E., Jüngling, E., Zitt, C., and Lückhoff, A. (2003) *Biochem. J.* **371,** 1045–1053
11. Brauchi, S., Orio, P., and Latorre, R. (2004) *Proc. Natl. Acad. Sci. U.S.A.* **101,** 15494–15499
12. Starkus, J., Beck, A., Fleig, A., and Penner, R. (2007) *J. Gen. Physiol.* **130,** 427–440
13. McHugh, D., Flemming, R., Xu, S. Z., Perraud, A. L., and Beech, D. J. (2003) *J. Biol. Chem.* **278,** 11002–11006
14. Heiner, I., Eisfeld, J., Warnstedt, M., Radukina, N., Jüngling, E., and Lückhoff, A. (2006) *Biochem. J.* **398,** 225–232
15. Chuang, H. H., Neuhausser, W. M., and Julius, D. (2004) *Neuron* **43,** 859–869
16. Rohács, T., Lopes, C. M., Michailidis, I., and Logothetis, D. E. (2005) *Nat. Neurosci.* **8,** 626–634
17. Kühn, F. J., Kühn, C., and Lückhoff, A. (2009) *J. Biol. Chem.* **284,** 4102–4111
18. Csanády, L., and Törocsik, B. (2009) *J. Gen. Physiol.* **133,** 189–203
19. Kühn, F. J., Knop, G., and Lückhoff, A. (2007) *J. Biol. Chem.* **282,** 27598–27609
20. Du, J., Xie, J., and Yue, L. (2009) *Proc. Natl. Acad. Sci. U.S.A.* **106,** 7239–7244
21. Andersson, D. A., Chase, H. W., and Bevan, S. (2004) *J. Neurosci.* **24,** 5364–5369
22. Bödding, M., Wissenbach, U., and Flockerzi, V. (2007) *Cell Calcium* **42,** 618–628
23. Hui, K., Guo, Y., and Feng, Z. P. (2005) *Biochem. Biophys. Res. Commun.* **333,** 374–382
24. Mahieu, F., Janssens, A., Gees, M., Talavera, K., Nilius, B., and Voets, T. (2010) *J. Physiol.* **588,** 315–324
25. Bezanilla, F. (2008) *Nat. Rev. Mol. Cell Biol.* **4,** 323–332
26. Swartz, K. J. (2008) *Nature* **456,** 891–897
27. Karashima, Y., Talavera, K., Everaerts, W., Janssens, A., Kwan, K. Y., Vennekens, R., Nilius, B., and Voets, T. (2009) *Proc. Natl. Acad. Sci. U.S.A.* **106,** 1273–1278
28. Long, S. B., Campbell, E. B., and Mackinnon, R. (2005) *Science* **309,** 903–908
29. Lu, Z., Klem, A. M., and Ramu, Y. (2002) *J. Gen. Physiol.* **120,** 663–676
30. Tong, Q., Zhang, W., Conrad, K., Mostoller, K., Cheung, J. Y., Peterson, B. Z., and Miller, B. A. (2006) *J. Biol. Chem.* **281,** 9076–9085
31. Mederos y Schnitzler, M., Wäring, J., Gudermann, T., and Chubanov, V. (2008) *FASEB J.* **22,** 1540–1551